DOI: 10.1002/cssc.200800099

Hangman Salen Platforms Containing Dibenzofuran Scaffolds

Jenny Y. Yang,[a] Shih-Yuan Liu,[a] Ivan V. Korendovych,[b] Elena V. Rybak-Akimova,[b] and Daniel G. Nocera*[a]

The synthesis of salen ligands bearing two rigid dibenzofuran spacers functionalized with carboxylic acid and benzoic acid groups completes a series of "Hangman" ligands with the acid functionalities differentially extended across the molecular cleft. Stopped-flow studies show that a high-valent metal oxo intermediate is produced at Hangman platforms when H_2O_2 is employed as a primary oxidant. The activity of this oxo species in promoting the disproportionation of hydrogen peroxide and olefin epoxidations is discussed in the context of the distance between the acid group and the metal center. The chemistry of the Hangman oxo complexes described here provides a roadmap for water-splitting chemistry.

Introduction

Proton-coupled electron transfer (PCET)[1–5] is a central mechanism for natural and synthetic systems that derive their function from bond-making and bond-breaking catalysis involving the oxygen atom.[6–9] PCET is crucial to radical generation and the transport of the tyrosine radical[10–14] and substrate oxidation at a variety of enzyme active sites.[10,15,16] This PCET-induced oxidation catalysis may be captured at synthetic active sites that "hang" an acid–base group over a redox platform.[17–19] For example, "Hangman" porphyrin systems are evocative of mono-oxygenase cofactors.[20,21] The high-valent metal oxo intermediate from which mono-oxygenase activity is derived is unmasked by shuttling a proton from the hanging acid–base group to a coordinated peroxide. A high-valent oxo is also furnished at Hangman salen and salophen platforms. With H_2O_2 as a substrate, the Hangman salen is able to drive the catalytic disproportionation of H_2O_2 to H_2O and O_2. A burgeoning interest in H_2O_2 as a substrate for this catalase activity arises from the growing realization of the efficacy of salen complexes as therapeutic agents of reactive oxygen species (ROS)[22–24] in animals[25,26] and human tissue.[27] The use of the Hangman salen or salophen platform is ideal when used in combination with H_2O_2 as an oxygen source because the hanging group enhances the association of the H_2O_2 within the molecular cleft and is able to deliver a proton efficiently to unmask the oxo and prevent deleterious side reactions.[28,29] To create a framework in which to understand the effects of pocket size and flexibility on the PCET reactivity of Hangman salens, we report here the synthesis of dibenzofuran Hangman salens (HSD* and H_{ph}SD*) and provide a comparative reactivity study of the HSD*/H_{ph}SD* and HSX*/H_{ph}SX* salen platforms (Figure 1). Moreover, intermediates important to catalysis were identified by stopped-flow studies of H_{ph}SX-OMe/H_{ph}SX-OMe systems (Figure 1). Our findings reveal that there is an optimum cleft size for substrate activation at Hangman salen platforms.

Results

Hangman salen compounds appended with a dibenzofuran scaffold were assembled according to the sequence described in Scheme 1. 4,6-Dibromodibenzofuran (**1**) was synthesized by dilithiation of the commercially available dibenzofuran using *sec*-butyllithium followed by bromination by elemental bromine.[30] To generate the carboxylic acid functionalized Hangman, 4,6-dibromodibenzofuran was monolithiated using phenyllithium and carbon dioxide was bubbled through the solution to form 4-bromo-6-hydroxycarbonyldibenzofuran (**2**).[30] Palladium-catalyzed Suzuki coupling with 3-*tert*-butyl-2-hydroxy-5-(4,4,5,5-tetramethyl-[1,3,2]dioxaborolan-2-yl)benzaldehyde[31] furnished the salen precursor **6**. Synthesis of the benzoic acid functionalized dibenzofuran required additional steps, similar to the multistep procedure used to obtain the analogous xanthene derivative.[19] 4,6-Dibromodibenzofuran (**1**) was monolithiated using phenyllithium, followed by addition of tributyltin chloride to give **3**. Addition of elemental iodine to **3** yields 4-bromo-6-iodobenzofuran (**4**). The aryl iodo position was selectively coupled under palladium-catalyzed Suzuki cross-coupling conditions with 4-methoxycarbonylphenylboronic acid to give **5**. The deprotected benzoic acid derivative of **5** could not be isolated cleanly due to its insolubility, but **5** can be coupled directly with 3-*tert*-butyl-2-hydroxy-5-(4,4,5,5-tetramethyl-[1,3,2]dioxaborolan-2-yl)benzaldehyde to give **7**. The

[a] *Dr. J. Y. Yang, Dr. S.-Y. Liu,[+] Prof. D. G. Nocera*
Department of Chemistry, Massachusetts Institute of Technology
77 Massachusetts Ave., Cambridge, MA 02139 (USA)
Fax: (+1) 617-253-7670
E-mail: nocera@mit.edu

[b] *I. V. Korendovych, Prof. E. V. Rybak-Akimova*
Department of Chemistry, Tufts University
62 Talbot Avenue, Medford, MA 02155 (USA)
Fax: (+1) 617-627-3443

[+] *Present address: Department of Chemistry, University of Oregon*
1253 University of Oregon, Eugene, OR 97403-1253 (USA)

Supporting information for this article is available on the WWW under http://dx.doi.org/10.1002/cssc.200800099.

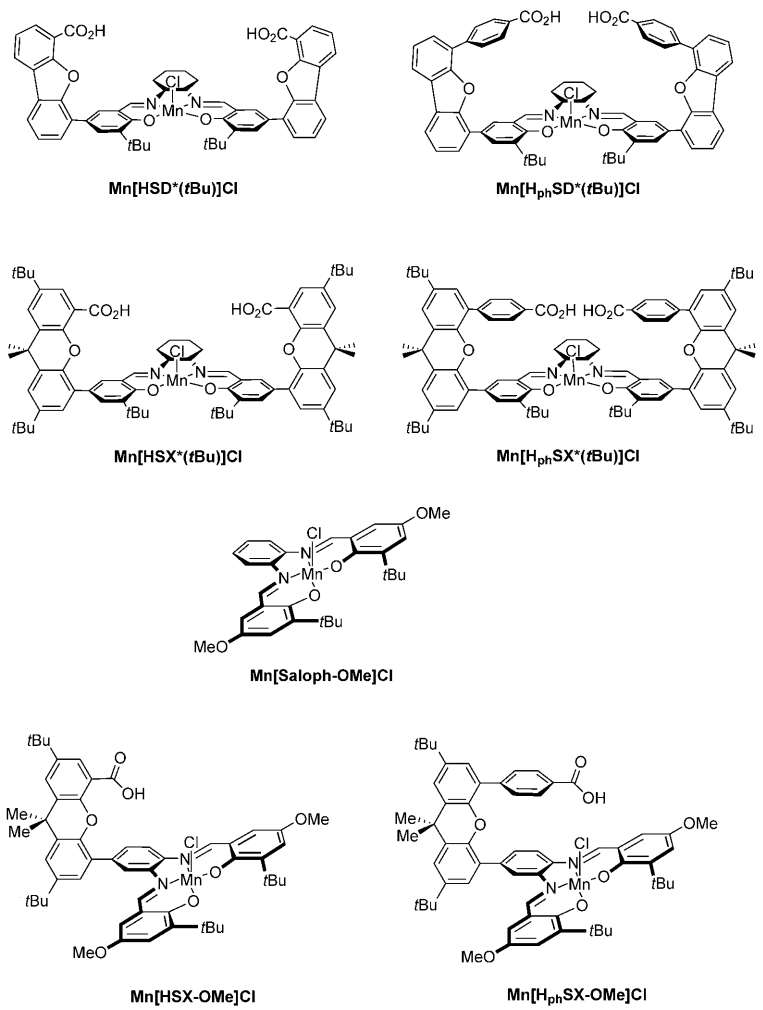

Figure 1. Structures of the dibenzofuran Hangman salens (HSD* and H_{ph}SD*), HSX*/H_{ph}SX* salen platforms, as well as Saloph and H_{ph}SX-OMe/H_{ph}SX-OMe systems.

methyl ester was easily deprotected using boron tribromide to afford **8**. Ligand precursors **6** and **8** were condensed with half an equivalent of (1*R*,2*R*)-(−)-1,2-diaminocyclohexane to furnish the ligand in good yields. Manganese(III) chloride was inserted by refluxing a solution of the ligand in ethanol with manganese (II) acetate in air, followed by workup with aqueous sodium chloride solution to give HSD **11** and **12**.

The reactivity of Hangman complexes **11** and **12** was evaluated for the catalase-like disproportionation of hydrogen peroxide. The amount of O_2 evolved for each catalyst, as provided by turnover numbers (TONs), is shown in Table 1. Of the two dibenzofuran Hangman complexes, **12** demonstrated greater activity. However, the reactivity of both DPD complexes is inferior to Hangman salen compounds with xanthene spacers, Mn[HSX**t*Bu]Cl and Mn[H_{ph}SX**t*Bu]Cl.

We have previously shown by using stopped-flow kinetics that a putative high-valent Mn^V oxo species is produced by treating Mn[H_{ph}SX-OMe]Cl with *meta*-chloroperbenzoic acid (*m*-CPBA) and iodosylbenzene, which are substrate models of H_2O_2.[29] H_2O_2 as a substrate, however, has heretofore not been examined by stopped-flow spectroscopy. Consequently, the nature of the intermediate produced from protonation of H_2O_2 within the Hangman cleft has not been established. Accordingly, stopped-flow studies of the reaction of H_2O_2 with Mn Hangman salens were undertaken; for comparative purposes, Mn[H_{ph}SX-OMe]Cl was chosen as the catalyst for these studies.

Figure 2 presents the transient spectrum obtained upon mixing a solution of H_2O_2 and a basic MeOH solution of Mn[H_{ph}SX-OMe]Cl. As can be seen from Figure 2, the reaction of Mn[H_{ph}SX-OMe]Cl with H_2O_2 results in a spectrum that features absorption maxima and the same isosbestic points as those observed for spectra generated by treating Mn[H_{ph}SX-OMe]Cl with *m*-CPBA (Figure 2b) or iodosylbenzene (Figure 2c). As expected, the absorption maxima of the transient species produced by H_2O_2 are not as pronounced as that produced for *m*-CPBA. In the case of *m*-CPBA, catalase activity (i.e., disproportionation of the peroxy substrate) is arrested thus permitting the Mn^V oxo intermediate to accrue over time. This is not the case for H_2O_2. The intermediate is available to react with a second molecule of H_2O_2 to complete the catalase reaction. Hence, the absorption maxima of the Mn^V oxo intermediate are not pronounced owing to the intrinsically lower concentration of the intermediate. For this reason, we emphasize the similarity of the isosbestic points across the substrate series as an indication of Mn^V oxo formation upon protonation of H_2O_2 within the Hangman cleft. The similarity between the spectra pro-

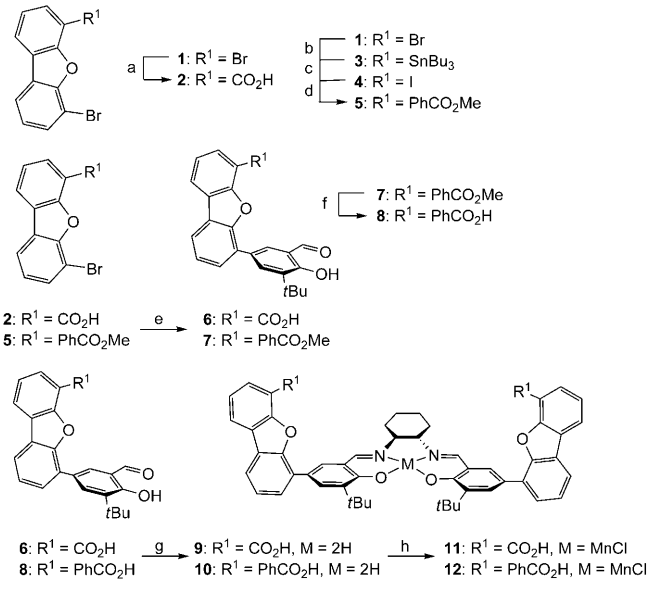

Scheme 1. Synthesis of Hangman salen compounds appended with a dibenzofuran scaffold. Reagents and conditions: a) 1) phenyllithium, cyclohexane/THF; 2) CO_2 gas; b) 1) phenyllithium, cyclohexane/THF; 2) $SnBu_3Cl$; c) I_2, CH_2Cl_2; d) 4-methoxycarbonylphenyboronic acid, CsF, [$Pd(PPh_3)_4$], dioxane; e) 3-*tert*-butyl-2-hydroxy-5-(4,4,5,5-tetramethyl-[1,3,2]dioxaborolan-2-yl)benzaldehyde, Na_2CO_3, [$Pd(PPh_3)_4$], DMF/H_2O; f) BBr_3, CH_2Cl_2; g) (1*R*,2*R*)-(−)-1,2-diaminocyclohexane, EtOH; h) 1) $Mn(OAc)_2{\cdot}4H_2O$, EtOH; 2) aq. NaCl.

Table 1. Observed turnover numbers for H_2O_2 disproportionation and epoxidation of 2,2-dimethylpropionic acid 4-vinylphenyl ester by manganese Hangman catalysts.

Catalyst	Turnover numbers (TONs)	
	disproportionation[a]	epoxidation[b]
Mn[H_{ph}SX*-*t*Bu]Cl	2495[c]	26
Mn[HSX*-*t*Bu]Cl	5328[c]	16
Mn[H_{ph}SX-*t*Bu]Cl	4372[d]	–
Mn[H_{ph}SX-OMe]Cl	4500	–
Mn[H_{ph}SD*-*t*Bu]Cl	2537	8
Mn[HSD*-*t*Bu]Cl	838	4
Mn[salen]Cl[e]	164[c]	8
Mn[salen]Cl[e]	182[c,f]	–

[a] In 2:1 dichloromethane/methanol at 25 °C over 1 h. [b] In dichloromethane with aqueous NaOCl at 25 °C over 3 h. [c] Data taken from Ref. [31]. [d] Data taken from Ref. [19]. [e] salen = (1*R*,2*R*)-(−)-[(1,2-cyclohexanediamino-*N*,*N*′-bis(3,5-di-*tert*-butylsalicylidene)]. [f] In the presence of two equivalents of benzoic acid.

duced by the reaction of Mn[H_{ph}SX-OMe]Cl with H_2O_2 and the *m*-CPBA and iodosylbenzene model substrates supports the contention that the Mn^V oxo species is produced initially from the reaction of H_2O_2 with Mn Hangman salen complexes.

The growth of the transient spectrum of Mn^V and the decay of the Mn^{III} reactant are simultaneously fit by a first-order exponential equation. The correspondence of these opposing kinetic processes indicates that additional intermediates do not form upon the cleavage of the O–O bond to generate Mn^V oxo. The first-order kinetics of Mn^V oxo formation is consistent with the observation of heterolysis of O–O bonds of peroxides at other metal centers.[32–34] Concentration-dependent studies show that the formation of the Mn^V oxo species is first order in Mn[H_{ph}SX-OMe]Cl and first order in H_2O_2; the rate constant for the formation of the Mn^V oxo is listed in Table 2 together with activation parameters as determined from measuring the rate constant over the temperature range 233–273 K.[35] The activation entropy, which is consistent with a transition state formed from a bimolecular reaction, is favorably affected by the Hangman architecture. The activation entropies for both the Mn[HSX-OMe]Cl and Mn[H_{ph}SX-OMe]Cl platforms are attenuated as compared to that of the Mn[Saloph-OMe]Cl parent complex, though we note that this entropic benefit of the Hangman motif is countered by a substantial increase in the activation enthalpy, thus leading to a slower reaction for the Mn Hangman complexes over the temperature range that we investigated. Moreover, as seen from Table 2, the production of the Mn^V oxo is not significantly affected by the presence or placement of the hanging group. The rate constants and activation parameters for the production of the Mn^V oxo vary marginally for a macrocycle lacking the acid–base group or one in which the acid–base group is extended by a phenyl spacer.

To examine the effect of the cleft geometry of Mn Hangman salen complexes (**11** and **12**) on H_2O_2 reaction chemistry, energy-minimized calculations on the hydroperoxide-bound species were performed. A simplified computational construct entailed the replacement of the cyclohexyldiamine bridge with ethylenediamine and the removal of *tert*-butyl and methyl

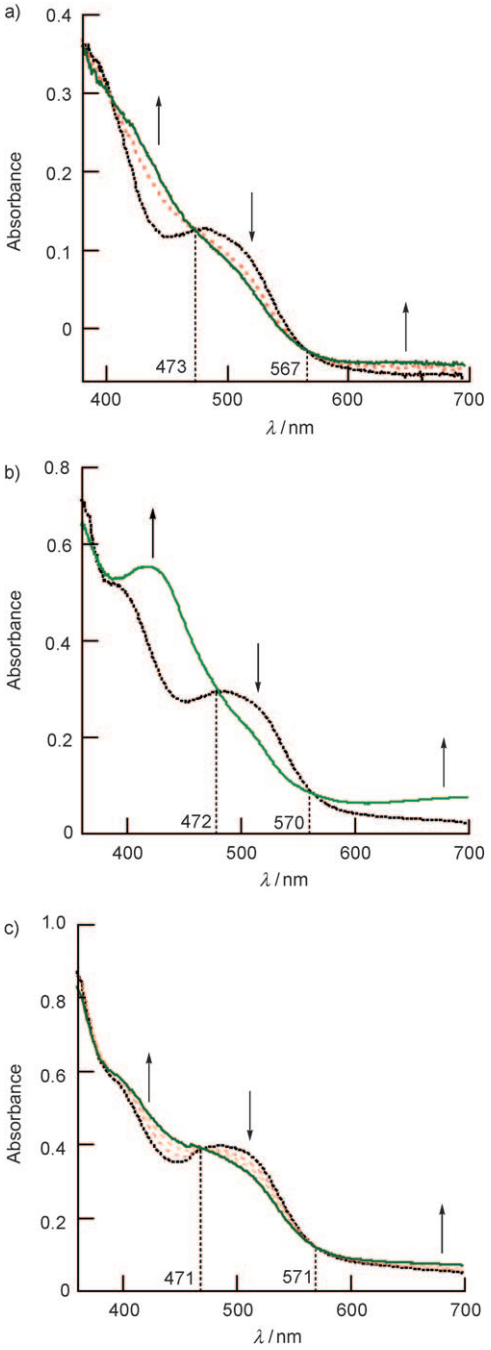

Figure 2. Absorption spectra from a stopped-flow reaction of 2.5×10^{-5} M Mn[H_{ph}SX-OMe]Cl (••••) in 2.5×10^{-4} M NaOH treated with a) 1.7×10^{-1} M H_2O_2 solution in MeOH at −50 °C, b) 3.3×10^{-4} M *m*-CPBA in 1:1 MeOH/MeCN at −20 °C, and c) 7.5×10^{-4} M iodosylbenzene in 1:1 MeOH/MeCN at 20 °C. The green solid line represents the appearance of the Mn^V species. The red dashed lines represent the transition from Mn^{III} to Mn^V.

groups from the macrocycle. Selected bond and distance measurements for those two compounds as well as the xanthene analogues are shown in Table 3. The dibenzofuran scaffold of **11** tilts the carboxylic acid functionalities vertically and laterally away from the bound hydroperoxide, giving an average acid-to-metal distance of about 7.4 Å (see Figure 3a). This distance can increase slightly with some rotation about the dibenzofuran–salen bond. As shown in Figure 3b for **12**, the car-

Table 2. Rate constants and activation parameters for the formation of an oxo intermediate[a] at Mn Hangman platforms upon treatment of the complex with H_2O_2.

Catalyst	k [$M^{-1}s^{-1}$][b]	$\Delta H^{\ddagger}$ [kcal mol^{-1}]	$\Delta S^{\ddagger}$ [kcal mol^{-1}]
Mn[HSX-OMe]Cl	4.5(2)	12.4(5)	−11(2)
Mn[H_{ph}SX-OMe]Cl	3.0(1)	12.9(5)	−9(2)
Mn[Saloph-OMe]Cl	29(2)	8.6(7)	−20(3)

[a] [Mn complex] = 2.5×10^{-5} M; [H_2O_2] = 0.17 M, [NaOH] = 2.5×10^{-4} M, and T = 273 K; standard deviations (in parentheses) determined from at least three experimental runs. [b] Rates at 273 K.

Table 3. Selected bond distance parameters from DFT calculated energy-minimized structures of the hydroperoxide complexes of manganese Hangman salen compounds.

	Distance [Å]			
	Mn(HSX*)OOH[a]	Mn(H_{ph}SX)*OOH[a]	Mn(HSD)*OOH	Mn(H_{ph}SD)*OOH
Mn–O	1.89	1.85	1.968	1.961
peroxide O–O	1.46	1.46	1.447	1.452
peroxide O–H	0.99	0.99	0.986	0.986
acid (H)O–Mn	5.14, 6.77	4.58, 6.03	7.338, 7.532	7.039, 7.568
	$H_{peroxide}$–$O(H)_{acid}$	$H_{peroxide}$–$O(C)_{acid}$	$H_{peroxide}$–$O(H)_{acid}$	$H_{peroxide}$–$O(H)_{acid}$
peroxide–acid	1.94	3.11	5.05	4.579

[a] Data taken from Ref. [35].

boxylic acid moves nearer to the Mn center in a lateral direction when a phenyl extension is incorporated into the framework. Opposing this lateral extension, the acid tilts upwards and moves further away vertically from the metal center. The net result is that the acid-to-metal distance in **12** of about 7.0 Å and 7.6 Å is similar to that of **11**. Unlike xanthene-modified salens, the dibenzofuran scaffold does not permit a convergent approach of the carboxylic acids and an intermolecular carboxylic acid dimer is not formed.

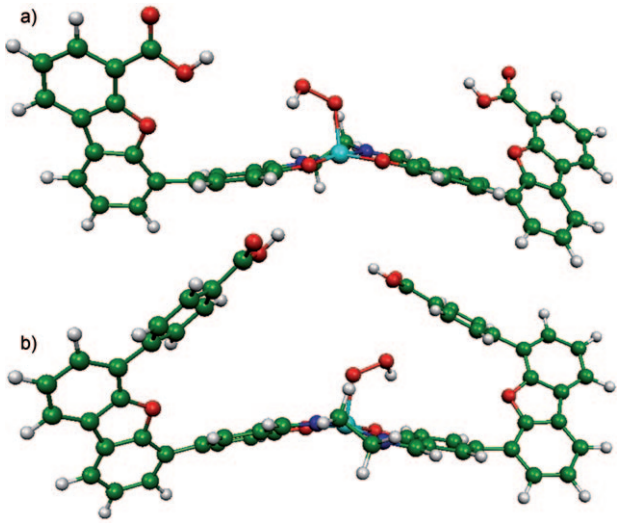

Figure 3. Energy-minimized structures obtained from DFT calculations of the hydroperoxide complexes a) Mn[HSD*tBu]OOH and b) Mn[H_{ph}SD*tBu]OOH (Mn turquoise, N blue, O red, C green, H white).

The availability of a Mn^{V} oxo presages an olefin oxidation chemistry. We sought to enhance olefin epoxidation activity by using olefins appended with a functional group capable of hydrogen bonding, thereby positioning the substrate over the Mn^{V} oxo. For this study, we examined the epoxidation of the substrate 2,2-dimethylpropionic acid 4-vinylphenyl ester using sodium hypochlorite as the oxidant. We turned to this oxidant as opposed to H_2O_2 because, upon the generation of Mn^{V} oxo, H_2O_2 will react with the Mn^{V} oxo before it is able to oxidize the olefinic substrate. Even when the concentration of H_2O_2 is kept low by adding it slowly using a syringe pump, olefin epoxidation is overwhelmed by H_2O_2 disproportionation and only low olefin epoxidation activity is observed using H_2O_2 as the oxidant. Conversely, as shown in Table 1, appreciable TONs for olefin epoxidation by Mn Hangman salen catalysts are observed for hypochlorite oxidants. The xanthene-based catalysts, Mn[H_{ph}SX*-tBu]Cl and Mn[HSX*-tBu]Cl, display the greatest TONs. The dibenzofuran Hangman salen analogues show approximately the same activity as that obtained for the unmodified control catalyst.

Discussion

Hydrogen peroxide, as a primary oxidant, furnishes a reactive Mn^{V} oxo intermediate at Hangman salen platforms. Stopped-flow studies establish that the Mn^{V} oxo is produced in a bimolecular reaction of H_2O_2 and the Hangman salen complex. Whereas protonation of a bound Mn^{III} peroxy group yields the Mn^{V} oxo in a single step, stopped-flow studies reveal that this protonation event is not enhanced by the presence of the acid–base hanging group of the Hangman architecture. Notwithstanding, comparative studies between nonfunctionalized Mn salens and Mn Hangman salens establish the criticality of the hanging acid–base group to catalytic turnover. Our results are consistent with the presence of the hanging group 1) to enhance catalysis by predisposing O–O bond cleavage by a heterolysis versus a homolysis pathway[28,36] and 2) affect a rate-determining step involving the reaction of a second equivalent of hydrogen peroxide with the Mn^{V} oxo intermediate by assisting in the assembly of that hydrogen peroxide in the molecular cleft.[19] These mechanistic considerations concur with computational predictions for the disproportionation of H_2O_2 by Mn salen catalysts. An energy landscape of the reaction profile shows that the end-on approach of the second equivalent of hydrogen peroxide appears to be the critical determinant of the oxidation kinetics[37] and not the proton-assisted formation of the Mn^{V} oxo.[38]

The dimension of the Hangman cleft plays a pivotal role in substrate assembly, thus providing insight on the disparate activity of the Hangman complexes. The increase in the acid dis-

tance of **12** occurs along a vector that is primarily perpendicular to the metallosalen macrocycle. This geometry is better able to accommodate the roughly linear binding of hydrogen peroxide and accordingly is consistent with **12** as a superior catalyst to **11**, which displays a hanging group that is displaced both vertically and horizontally. The enhanced catalytic epoxidation of olefins containing a hydrogen-bonding functionality, which can interact with the carboxylic acid groups, suggests that substrate pre-assembly within the Hangman cleft may also contribute to enhanced TONs.

Control of the secondary coordination environment has connotations to sustainability that extend beyond biomimetic and organic "green" oxidation reactions. The production of an epoxide at the Mn Hangman salen platform entails nucleophilic attack of a two-electron donor on a reactive oxo intermediate. In doing so, two new C–O bonds are formed with the release of the oxygen atom from the metal center. It is precisely this type of transformation that has been postulated in the water-splitting reaction of Photosystem II. The appearance of the structures of the Photosystem II suggest various possibilities, shown in Figure 3, for O_2 generation from the S4 Kok state[39] of the oxygen-evolving complex (OEC).[40–43] Oxygen generation is proposed to arise from oxos associated with a highly oxidized $\{Mn_4Ca\}$ cluster.[44,45] In one formalism, a d^2 metal-oxo is posited as the intermediate in O_2 generation. If all the oxidizing equivalents are borne by the Mn centers, a $\{Mn^{IV}Mn^{V}\}$ core is obtained. In this case, an electrophilic oxo at the "dangler" Mn^V center[46] of OEC is proposed to be attacked by a nucleophilic hydroxide to form the O–O bond.[47,48] In drawing a chemical parallel to epoxidation, an oxygen atom replaces the two carbon atoms in olefin epoxidation. Hence, the transformation of epoxide to an olefin at a metal oxo is a close functional relative to the water-splitting problem. To this end, the Hangman strategy is intriguing owing to the ability of the platform to noncovalently assemble substrate molecules proximate to the oxo. We have already shown the utility of the hanging group to assemble water in the second coordination sphere,[17] akin to the pre-organization that is postulated at the active site of OEC.[6,47] To effect water splitting, the olefinic nucleophile of the reaction described here needs to be replaced by hydroxide. Practically, OH^- is thermodynamically more difficult to oxidize than olefins and hence it will be necessary to maximize the electrophilicity of the oxo.

Conclusion

The supply of secure, clean, sustainable energy is arguably the most important scientific and technical challenge facing humanity in the 21st century.[49–52] The imperative for the discipline of chemistry is to meet this energy need in a sustainable and environmentally responsible way. The chemistry of the Hangman oxo described here provides a roadmap for water-splitting chemistry. Studies centered at replacing H_2O_2 and olefin substrates with water within the cleft of Hangman metal-oxo platforms are currently underway.

Experimental Section

Materials and Methods: Silica gel 60 (70–230 and 230–400 mesh) was used for column chromatography. Analytical thin layer chromatography was performed using F254 silica gel (precoated sheets, 0.2-mm thick). Solvents for synthesis were reagent grade or better and used as received or dried according to standard methods.[53] 3-*tert*-Butyl-2-hydroxybenzaldehyde, potassium acetate, and (1*R*,2*R*)-(−)-1,2-diaminocyclohexane were used as received from Aldrich. Bis(pinacolato)diboron was used as received from Frontier Scientific. Bis(tricyclohexylphosphine)palladium, tetrakis(triphenylphosphine)palladium, sodium carbonate, and manganese(II) acetate tetrahydrate were used as received from Strem Chemicals. For stopped-flow experiments, MeOH (anhydrous, Aldrich) and aqueous hydrogen peroxide (Alfa Aesar; 30%) were used as received. 3-Chloroperoxybenzoic acid (*m*-CPBA) was purchased from Aldrich (77%) and purified by washing with pH 7.40 phosphate buffer and recrystallization from pentane to remove 3-chlorobenzoic acid. Purity (>95%) was determined by ^{1}H NMR spectroscopy. The 30% aqueous solution of hydrogen peroxide was used as received from Alfa Aesar. The hydrogen peroxide was volumetrically determined to be 10.4 M (32%) through its decomposition to oxygen gas over manganese dioxide. The following compounds were obtained using published protocols and their purity was confirmed by ^{1}H NMR spectroscopy: 4,6-dibromodibenzofuran (**1**),[54] 4-bromo-6-hydroxycarbonyldibenzofuran (**2**),[54] 3-*tert*-butyl-2-hydroxy-5-(4,4,5,5-tetramethyl-[1,3,2]dioxaborolan-2-yl)benzaldehyde,[55] 4-methoxycarbonyl-5-bromo-2,7-di-*tert*-butyl-9,9-dimethylxanthene,[56] HSX*tBu,[55] H_{ph}SX*tBu[55], and [H_{ph}SX-OMe].[57] The corresponding MnCl complexes Mn[HSX*tBu]Cl,[55] Mn[H_{ph}SX*tBu]Cl,[55] and Mn[H_{ph}SX-OMe]Cl[57] were prepared as previously reported and their purity was confirmed by mass spectroscopy and elemental analysis. ^{1}H NMR spectra were measured on solutions in $CDCl_3$ or C_4D_8O (Cambridge Isotope Laboratories) at the MIT Department of Chemistry Instrumentation Facility (DCIF) using an Inova 500 Spectrometer at 25 °C. All chemical shifts are reported using the standard δ notation in parts per million relative to tetramethylsilane, and spectra were internally calibrated to the monoprotio impurity of the deuterated solvent used. High-resolution mass spectrometry (HRMS) analyses were carried out by the MIT Department of Chemistry Instrumentation Facility on a Bruker APEXIV47e.FT-ICR-MS using an Apollo ESI source.

(6-Bromodibenzofuran-4-yl)tributylstannane (**3**): A solution of 4,6-dibromodibenzofuran (**1**; 0.500 g, 1.53 mmol) in dry THF (40 mL) was cooled in an acetone/dry ice bath under nitrogen. Phenyllithium (1.1 mL, 1.7 M solution in cyclohexane) was added, and the resulting solution was stirred for 30 min and then warmed to room temperature and stirred for an additional 30 min before the addition of tributyltin chloride (0.549 g, 1.69 mmol). After 15 min, the solvent was removed by rotary evaporation to reveal an oily residue. Pentane (15 mL) was added to the oil, and the solution was filtered. The filtrate was reduced by rotary evaporation and purified by column chromatography (silica gel, pentane) to give the desired product as an oil at room temperature (0.592 g, 72% yield). ^{1}H NMR (500 MHz, $CDCl_3$, 25 °C): δ = 7.94 (d, J = 8 Hz, 1H), 7.90 (d, J = 7.5 Hz, 1H), 7.66 (m, 2H), 7.43 (t, J = 8 Hz, 1H), 7.23 (t, J = 8 Hz, 1H), 1.76 (m, 6H), 1.48 (sextet, J = 7.5 Hz, 6H), 1.39 (t, J = 8 Hz, 6H), 1.00 ppm (t, J = 7.5 Hz, 9H). ^{13}C NMR (500 MHz, $CDCl_3$): δ = 162.21, 153.29, 135.69, 129.70, 126.35, 124.23, 123.66, 123.41, 122.16, 121.08, 119.73, 104.72, 29.41, 27.65, 13.98, 10.29 ppm.

4-Bromo-6-iododibenzofuran (**4**): Iodine (0.280 g, 1.75 mmol) was slowly added to a rapidly stirring solution of **3** (0.592 g, 1.10 mmol) dissolved in dichloromethane (10 mL). Upon stirring for 1 h, the so-

lution was washed with saturated aqueous sodium carbonate solution (2×10 mL) followed by deionized water (10 mL). The organic portion was dried over $MgSO_4$, and the solvent was removed by rotary evaporation to reveal an oily solid which was purified by loading onto a short silica plug and eluting with pentane and then dichloromethane. The product was revealed as a colorless solid (0.386 g, 94%). ^{1}H NMR (500 MHz, $CDCl_3$, 25 °C): δ = 7.90 (d, J = 8 Hz, 1H), 7.87 (m, 2H), 7.66 (d, J = 8 Hz, 1H), 7.26 (dt, J = 8 Hz, 2.5 Hz, 1H), 7.15 ppm (dt, J = 5.5 Hz, 2.5 Hz, 1H). ^{13}C NMR (500 MHz, $CDCl_3$): δ = 153.06, 136.89, 130.88, 126.16, 125.08, 124.70, 124.57, 121.14, 120.32, 105.05, 75.82 ppm. HRMS (ESI): *m/z* calcd for $C_{12}H_6BrIONa$ $[M+Na]^+$: 394.8539; found: 394.8542.

4-(6-Bromodibenzofuran-4-yl)benzoic acid methyl ester (**5**): Under nitrogen, a mixture of **4** (0.250 g, 0.670 mmol), 4-methoxycarbonylphenylboronic acid (0.133 g, 0.737 mmol), cesium fluoride (0.336 g, 2.21 mmol) and tetrakis(triphenylphosphine)palladium (0.077 g, 0.067 mmol) were added to dimethoxyethane (8 mL) and heated to 90 °C for 24 h. Upon cooling to room temperature, the solvent was removed under vacuum and the residue was taken up in dichloromethane (50 mL) and washed with deionized water (2× 10 mL). The organic portion was dried with $MgSO_4$, and the solvent was removed by rotary evaporation. The residue was purified by column chromatography (silica gel, 7:3 dichloromethane/pentane) to reveal a colorless product (0.235 g, 92%). ^{1}H NMR (500 MHz, $CDCl_3$, 25 °C): δ = 8.21 (d, J = 8.5 Hz, 2H), 8.04 (d, J = 8.5 Hz, 2H), 7.90 (dd, J = 7.5 Hz, 1 Hz, 1H), 7.87 (dd, J = 7.5 Hz, 1 Hz, 1H), 7.66 (dd, J = 7.5 Hz, 1 Hz, 1H), 7.61 (dd, J = 7.5 Hz, 1 Hz, 1H), 7.43 (t, J = 7.5 Hz, 1H), 7.22 (t, J = 7.5 Hz, 1H), 3.98 ppm (s, 3H). ^{13}C NMR (500 MHz, $CDCl_3$): δ = 166.99, 153.29, 153.09, 140.40, 130.30, 130.01, 129.34, 128.59, 127.33, 125.38, 125.14, 124.80, 124.19, 123.84, 120.94, 119.72, 104.68, 52.23 ppm. HRMS (ESI): *m/z* calcd for $C_{20}H_{14}BrO_2$ $[M+H]^+$: 381.0121; found: 381.0130.

6-(3-*tert*-Butyl-5-formyl-4-hydroxyphenyl)dibenzofuran-4-carboxylic acid (**6**): Under nitrogen, a mixture of 4-bromo-6-hydroxycarbonyldibenzofuran (**2**; 0.200 g, 0.687 mmol), 3-*tert*-butyl-2-hydroxy-5-(4,4,5,5-tetramethyl-[1,3,2]dioxaborolan-2-yl)benzaldehyde (0.230 g, 0.756 mmol), sodium carbonate (0.106 g, 1.03 mmol), and tetrakis-(triphenylphosphine)palladium (0.048 g, 0.041 mmol) in *N*,*N*-dimethylformamide (DMF, 14.5 mL) and deionized water (1.5 mL) was heated at 90 °C for 36 h. Upon cooling, the reaction mixture was extracted with dichloromethane (3×20 mL). The combined organic layers were then washed with water (2×20 mL) and dried over $MgSO_4$, and the solvent was removed by rotary evaporation. The residue was purified by column chromatography (8:2 pentane/ethyl acetate) to reveal the colorless product (0.125 g, 47% yield). ^{1}H NMR (500 MHz, C_4D_8O, 25 °C): δ = 12.08 (s, 1H), 10.06 (s, 1H), 8.40 (d, J = 2 Hz, 1H), 8.37 (d, J = 2 Hz, 1H), 8.29 (dd, J = 7.5 Hz, 1 Hz, 1H), 8.13 (dd, J = 7.5 Hz, 1 Hz, 1H), 8.03 (dd, J = 7.5 Hz, 1 Hz, 1H), 7.80 (dd, J = 7.5 Hz, 1 Hz, 1H), 7.47 (m, 2H), 1.56 ppm (s, 9H). ^{13}C NMR (500 MHz, C_4H_8O): δ = 198.13, 164.97, 160.67, 154.99, 153.44, 137.98, 134.22, 132.49, 129.79, 127.10, 125.94, 125.76, 125.18, 124.38, 124.26, 123.79, 122.59, 121.28, 119.49, 116.25, 35.04, 28.93 ppm. HRMS (ESI): *m/z* calcd for $C_{24}H_{20}O_5Na$ $[M+Na]^+$: 411.1208; found: 411.1202.

4-[6-(3-*tert*-Butyl-5-formyl-4-hydroxyphenyl)dibenzofuran-4-yl]benzoic acid methyl ester (**7**): Under nitrogen, a mixture of **5** (0.250 g, 0.656 mmol), 3-*tert*-butyl-2-hydroxy-5-(4,4,5,5-tetramethyl-[1,3,2]dioxaborolan-2-yl)benzaldehyde (0.219 g, 0.721 mmol), sodium carbonate (0.101 g, 0.984 mmol), and tetrakis(triphenylphosphine)palladium (0.045 g, 0.039 mmol) in DMF (9 mL) and deionized water (1 mL) was heated at 90 °C for 24 h. Upon cooling, the reaction mixture was extracted with dichloromethane (3×20 mL). The combined organic layers were then washed with water (2×20 mL) and dried over $MgSO_4$, and the solvent was removed by rotary evaporation. The residue was purified by column chromatography (7:3 dichloromethane/pentane) to reveal the colorless product (0.238 g, 76% yield). ^{1}H NMR (500 MHz, $CDCl_3$, 25 °C): δ = 11.91 (s, 1H), 9.97 (s, 1H), 8.16 (d, J = 9 Hz, 2H), 8.10 (d, J = 2 Hz, 1H), 8.03 (dd, J = 9 Hz, 1 Hz, 1H), 7.97 (m, 4H), 7.68 (dd, J = 7.5 Hz, 1 Hz, 1H), 7.63 (dd, J = 7.5 Hz, 1 Hz, 1H), 7.49 (quartet, J = 7.5 Hz, 2H), 3.98 (s, 3H), 1.44 ppm (s, 9H). ^{13}C NMR (500 MHz, $CDCl_3$): δ = 197.47, 167.01, 161.10, 153.42, 141.03, 138.84, 134.81, 132.07, 130.08, 129.52, 128.86, 128.74, 127.52, 127.15, 126.47, 125.21, 125.02, 124.95, 124.88, 123.84, 123.75, 121.06, 121.02, 120.87, 119.97, 119.84, 52.44, 35.25, 29.32 ppm. HRMS (ESI): *m/z* calcd for $C_{31}H_{26}O_5Na$ $[M + Na]^+$: 501.1672; found: 501.1678.

4-[6-(3-*tert*-Butyl-5-formyl-4-hydroxyphenyl)dibenzofuran-4-yl]benzoic acid (**8**): Under nitrogen, methyl ester **7** (0.080 g, 0.167 mmol) was dissolved in dry dichloromethane (6 mL) and the solution was cooled to 0 °C in an ice bath. A solution of 1.0 M boron tribromide (0.50 mL, 0.502 mmol) was added via syringe, and the reaction mixture was warmed to room temperature and stirred for 2 h, upon which deionized water (10 mL) was added. The subsequent mixture was extracted with dichloromethane (3×20 mL), and the combined organic layers were washed with fresh deionized water (10 mL) and than dried over $MgSO_4$. The solvent was removed by rotary evaporation. The residue was purified by column chromatography (99:1 dichloromethane/methanol) to reveal the colorless product (0.046 g, 59% yield). ^{1}H NMR (500 MHz, C_4D_8O, 25 °C): δ = 12.10 (s, 1H), 11.48 (bs, 1H), 10.04 (s, 1H), 8.16 (m, 4H), 8.11 (dd, J = 7.5 Hz, 1 Hz, 1H), 8.06 (m, 3H), 7.77 (dd, J = 7.5 Hz, 1 Hz, 1H), 7.71 (dd, J = 7.5 Hz, 1 Hz, 1H), 7.50 (m, 2H), 1.44 ppm (s, 9H). ^{13}C NMR (500 MHz, C_4D_8O): δ = 198.96, 167.64, 161.68, 154.31, 154.18, 141.43, 139.10, 135.22, 133.14, 131.50, 131.04, 129.45, 128.53, 128.00, 127.40, 126.12, 125.90, 125.82, 124.73, 124.68, 122.31, 121.68, 120.70, 35.89, 29.75 ppm. HRMS (ESI): *m/z* calcd for $C_{30}H_{25}O_5$ $[M+H]^+$: 465.1696; found: 465.1691.

H_2[HSD**t*Bu-COOH] (**9**): A mixture of carboxylic acid **6** (30.0 mg, 0.077 mmol) and (1*R*,2*R*)-(−)-1,2-diaminocyclohexane (4.4 mg, 0.039 mmol) was added to absolute ethanol (6 mL). The solution was heated at reflux for 2 h, and upon cooling the solvent was removed by rotary evaporation. The yellow residue was washed with cold methanol (0.3 mL) and dried under vacuum to give the product (30 mg, 91% yield). HRMS (ESI): *m/z* calcd for $C_{54}H_{51}N_2O_8$ $[M+H]^+$: 855.3640; found: 855.3631. Elemental analysis (%) calcd for $C_{54}H_{50}N_2O_8$: C 75.86, H 5.89, N 3.28; found: C 75.73, H 6.01, N 2.45.

H_2[H_{ph}SD**t*Bu-COOH] (**10**): A mixture of benzoic acid **8** (42.0 mg, 0.090 mmol) and (1*R*,2*R*)-(−)-1,2-diaminocyclohexane (5.2 mg, 0.045 mmol) was added to absolute ethanol (6 mL). The solution was heated to reflux for 2 h, and upon cooling the solvent was removed by rotary evaporation. The bright yellow residue was washed with cold methanol (0.5 mL) and dried under vacuum to give the product (36 mg, 80% yield). HRMS (ESI): *m/z* calcd for $C_{66}H_{59}N_2O_8$ $[M+H]^+$: 1007.4266; found: 1007.6217. Elemental analysis (%) calcd for $C_{66}H_{58}N_2O_8$: C 78.71, H 5.80, N 2.78; found: C 78.52, H 6.00, N 2.85.

Mn[HSD**t*Bu-COOH]Cl (**11**): A mixture of **9** (30.0 mg, 0.035 mmol) and manganese(II) acetate tetrahydrate (13.0 mg, 0.053 mmol) in absolute ethanol (4 mL) was heated at reflux for 2 h. Upon cooling, saturated aqueous sodium chloride (4 mL) was added, the solution was stirred for 20 min, and the solid was collected by filtration and washed with water. Upon drying, the brown solid was taken up in

dichloromethane and filtered. The filtrate was reduced to give the brown product (14 mg, 42% yield). HRMS (ESI): *m/z* calcd for $C_{54}H_{48}MnN_2O_8$ $[M-Cl]^+$: 907.2792; found: 907.2821. Elemental analysis (%) calcd for $C_{54}H_{48}ClMnN_2O_8$: C 68.75, H 5.13, N 2.97; found: C 68.66, H 5.23, N 2.85.

Mn[H_{ph}SD*tBu-COOH]Cl (**12**): A mixture of **10** (30.0 mg, 0.030 mmol) and manganese(II) acetate tetrahydrate (11.0 mg, 0.045 mmol) in absolute ethanol (6 mL) was heated at reflux for 2 h. Upon cooling, saturated aqueous sodium chloride (4 mL) was added, the solution was stirred for 20 min, and the solid was collected by filtration and washed with water. Upon drying, the brown solid was taken up in tetrahydrofuran and filtered. The filtrate was reduced to give the brown product (30 mg, 91% yield). HRMS (ESI): *m/z* calcd for $C_{66}H_{56}MnN_2O_8$ $[M-Cl]^+$: 1059.3423; found: 1059.3457. Elemental analysis (%) calcd for $C_{66}H_{56}ClMnN_2O_8$: C 72.36, H 5.15, N 2.56; found: C 72.16, H 5.26, N 2.43.

Mn[HSX-OMe]Cl (**16**): The complex was synthesized according to the reaction sequence shown in Scheme 2. In air, [Pd(dppf)]Cl_2 (30 mg, 0.041 mmol), 4-methoxycarbonyl-5-bromo-2,7-di-*tert*-butyl-

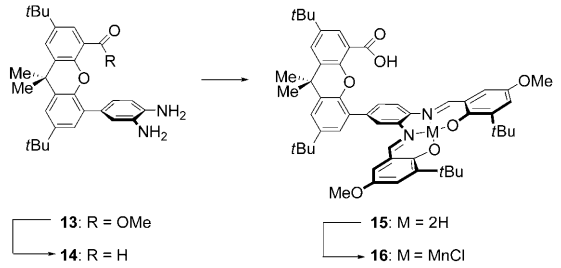

Scheme 2. Synthesis of the complex Mn[HSX-OMe]Cl (**16**).

9,9-dimethylxanthene (186 mg, 0.405 mmol), 4-(4,4,5,5-tetramethyl[1,3,2]-dioxaborolan-2-yl)benzene-1,2-diamine (133 mg, 0.567 mmol), and K_2CO_3 (280 mg, 2.00 mmol) were added to an oven-dried Schlenk tube equipped with a stir bar. The Schlenk tube was fitted with a rubber septum, evacuated, and then refilled with argon. A mixture of dioxane (3.8 mL) and degassed water (0.8 mL) was added via syringe, and the reaction mixture was stirred at 100 °C for 21 h. At the conclusion of the reaction, the mixture was diluted with diethyl ether, filtered through a pad of silica gel with copious washings (3:2 Et_2O/THF), concentrated, and purified by column chromatography (3:2 Et_2O/THF). The combined fractions were concentrated to dryness, and the residue washed thoroughly with pentane. The desired product **13** was obtained as a white solid (108 mg, 55%). ^{1}H NMR (500 MHz, CD_2Cl_2): δ = 7.58 (d, J = 2.5 Hz, 1H), 7.49 (d, J = 2.0 Hz, 1H), 7.37 (d, J = 2.5 Hz, 1H), 7.23 (d, J = 2.5 Hz, 1H), 7.02 (d, J = 1.5 Hz, 1H), 6.85 (dd, J = 8.0 Hz, J = 2.0 Hz, 1H), 6.75 (d, J = 8.0 Hz, 1H), 3.59 (s, 3H), 3.50 (br, 4H), 1.67 (s, 6H), 1.35 (s, 9H), 1.33 ppm (s, 9H). ^{13}C NMR (125 MHz, CD_2Cl_2): δ = 168.5, 147.6, 146.3, 145.6 (x2), 134.7, 134.6, 131.6, 130.5, 130.3, 129.9, 126.6, 126.4, 125.6, 121.8, 121.4, 120.7, 119.2, 116.3, 52.4, 35.5, 35.0, 34.9, 32.2, 31.8, 31.6 ppm. FTIR (thin film): $\tilde{\nu}$ = 3334, 2961, 2905, 2868, 1709, 1624, 1586, 1518, 1481, 1448, 1394, 1363, 1247, 1212 cm^{-1}. HRMS (ESI): *m/z* calcd for $C_{31}H_{38}N_2O_3$ $[M+H]^+$: 487.2955; found: 487.2966.

A vial containing a stir bar was charged with a solution of **13** (100 mg, 0.205 mmol) in THF (1.0 mL). A solution of NaOH (1.00 mL, 3.00 mmol; 3.0 M solution in water) was added. The vial was sealed with a Teflon cap, and the reaction was allowed to stir at 100 °C for 60 min. At the conclusion of the reaction, water was added and the resulting precipitate was collected on a glass frit. This crude material was dissolved in CH_2Cl_2, and a solution of HCl (2 N in water) was then added until the aqueous solution became acidic. The organic layer was separated from the aqueous phase, washed with brine, dried over Na_2SO_4, and concentrated under vacuum. This material was purified by column chromatography (5:1 CH_2Cl_2/MeOH), and the desired compound **14** was obtained as an off-white apparently air-sensitive solid (54 mg, 56%). HRMS (ESI): *m/z* calcd for $C_{30}H_{36}N_2O_3$ $[M+H]^+$: 473.2799; found: 473.2802.

A vial containing a stir bar was charged with **14** (54.0 mg, 0.114 mmol) and 3-*tert*-butyl-2-hydroxy-5-methoxybenzaldehyde (52.2 mg, 0.251 mmol). Ethanol (2.0 mL) was added, the vial was sealed with a Teflon cap, and the reaction mixture was allowed to stir at 100 °C for 19 h. The mixture was concentrated to dryness, and the resulting material was purified by column chromatography (CH_2Cl_2/Et_2O gradient) to afford the desired ligand **15** as a yellow solid (43 mg, 44%). ^{1}H NMR (500 MHz, CD_2Cl_2): δ = 13.4 (s, 1H), 8.79 (s, 1H), 8.74 (s, 1H), 8.02 (d, J = 2.5 Hz, 1H), 7.74 (d, J = 2.5 Hz, 1H), 7.55 (d, J = 2.5 Hz, 1H), 7.50 (dd, J = 8.5 Hz, J = 2.5 Hz, 1H), 7.46 (d, J = 7.5 Hz, 1H), 7.40 (d, J = 2.0 Hz, 1H), 7.35 (d, J = 2.5 Hz, 1H), 7.05 (d, J = 3.0 Hz, 1H), 7.02 (d, J = 3.0 Hz, 1H), 6.83 (d, J = 3.0 Hz, 1H), 6.76 (d, J = 3.0 Hz, 1H), 3.79 (s, 3H), 3.75 (s, 3H), 1.75 (s, 6H), 1.43 (s, 9H), 1.42 (s, 9H), 1.39 (s, 9H), 1.35 ppm (s, 9H). ^{13}C NMR (125 MHz, CD_2Cl_2): δ = 165.7, 165.2, 165.0, 156.0, 155.9, 152.10, 152.08, 148.4, 148.0, 147.2, 144.7, 143.5, 142.5, 139.9, 139.8, 137.5, 131.7, 130.5, 129.04, 129.00, 128.96, 128.87, 126.9 (2x), 123.0, 121.6, 120.6, 120.4, 120.3, 119.01, 118.96, 112.6, 112.4, 56.21, 56.19, 35.51, 35.49, 35.2, 35.1, 32.1, 31.8, 31.5, 29.6, 29.4 ppm. FTIR (thin film): $\tilde{\nu}$ = 2960, 2871, 1735, 1698, 1618, 1587, 1448, 1431, 1393, 1363, 1333, 1271, 1241, 1212, 1151, 1060 cm^{-1}. HRMS (ESI): *m/z* calcd for $C_{54}H_{64}N_2O_7$ $[M+H]^+$: 853.4686; found: 853.4775.

A vial containing a stir bar was charged with **15** (31 mg, 0.036 mmol) and $Mn(OAc)_2 \cdot 4H_2O$ (10 mg, 0.040 mmol). Ethanol (1.0 mL) was added and the reaction mixture was stirred at room temperature for 21 h. The dark brown reaction mixture was diluted with CH_2Cl_2. The organic extract was washed with brine, dried over Na_2SO_4, and concentrated under vacuum. The crude material was purified by column chromatography (CH_2Cl_2/Et_2O/MeOH gradient), and the desired compound **16** was obtained as a brown solid (28 mg, 82%). HRMS (ESI): *m/z* calcd for $C_{54}H_{62}N_2O_7MnCl$ $[M-Cl]^+$: 905.3922; found: 905.3930.

Dimethylpropionic acid 4-bromophenyl ester (**17**): 4-Bromophenol (1.00 g, 5.78 mmol) was dissolved in dry dichloromethane (20 mL). Pyridine (0.93 mL, 11.56 mmol) was added via syringe, followed by pivaloyl chloride (1.42 mL, 11.56 mmol), and the reaction mixture was stirred for 24 h. Deionized water (20 mL) was added to quench the reaction, and the separated aqueous layer was extracted with dichloromethane (2×20 mL). The combined organic layers were dried over $MgSO_4$, and the solvent was removed by rotary evaporation. The residue was purified by column chromatography (silica gel, gradient 2:8 pentane/dichloromethane to dichloromethane) to elute the product (1.40 g, 94% yield). ^{1}H NMR (500 MHz, $CDCl_3$): δ = 7.49 (dd, J = 9 Hz, 5 Hz, 2H), 6.96 (dd, J = 9H, 1.5 Hz, 2H), 1.35 ppm (s, 9H). HRMS (ESI): *m/z* calcd for $NaC_{13}H_{16}O_2$ $[M+Na]^+$: 227.1043; found: 227.1043.

2,2-Dimethylpropionic acid 4-vinylphenyl ester (**18**): Under nitrogen, a mixture of ester **17** (0.500 g, 1.94 mmol), tri(butyl)vinyltin (0.762 g, 2.05 mmol), and tetrakis(triphenylphosphine)palladium (0.450 g, 0.39 mmol) in toluene (8 mL) was heated at 110 °C in a sealed bomb for 12 h. Upon cooling, dichloromethane (50 mL) was added and the solution was washed with deionized water (2× 10 mL) and dried using $MgSO_4$. The solvent was removed by rotary evaporation, and the residue was purified by column chromatography (silica gel, 9:1 pentane/dichloromethane) to yield the colorless

product (0.351 g, 88% yield). ^{1}H NMR (300 MHz, $CDCl_3$): $\delta = 7.45$ (d, $J = 8.4$ Hz, 2H), 7.07 (dd, $J = 6.9$ Hz, 1.8 Hz, 2H), 6.74 (dd, $J = 17.8$ Hz, 10.8 Hz, 1H), 5.75 (dd, $J = 17.8$ Hz, 0.6 Hz, 1H), 5.28(dd, $J = 17.8$ Hz, 0.6 Hz, 1H), 1.42 ppm (s, 9H). ^{13}C NMR (500 MHz, $CDCl_3$): $\delta = 177.12$, 150.78, 136.05, 135.22, 127.22, 121.92, 121.67, 113.96, 39.18, 27.25 ppm.

2,2-Dimethylpropionic acid 4-oxiranylphenyl ester: A 0.05 M solution of Na_2HPO_4 (5 mL) was added to commercial bleach (Clorox, 12.5 mL), and this solution was added to a mixture of **18** (0.150 g, 0.68 mmol) and manganese(salophen) chloride (25 mg, 0.04 mmol) in dichloromethane (10 mL) and stirred for 3 h. The solution was extracted with dichloromethane (3×10 mL), and the organic layers were combined and dried using $MgSO_4$. The solvent was removed by rotary evaporation, and the remaining residue was purified by column chromatography (silica gel 3:7 pentane/dichloromethane) to elute the product (0.45 g, 31% yield). ^{1}H NMR (500 MHz, $CDCl_3$): $\delta = 7.29$ (d, $J = 8.5$ Hz, 2H), 7.04 (d, $J = 8.5$, 2H), 3.87 (t, $J = 2$ Hz, 1H), 3.15 (dd, $J = 5$ Hz, 4 Hz, 1H), 2.78 (dd, $J = 5$ Hz, 2 Hz, 1H), 1.36 ppm (s, 9H). ^{13}C NMR (500 MHz, $CDCl_3$): $\delta = 177.26$, 156.10, 135.11, 126.67, 121.85, 52.17, 52.49, 27.31. ppm. HRMS (ESI): *m/z* calcd for $NaC_{13}H_{16}O_3$ $[M+Na]^+$: 243.0992; found: 243.0998.

DFT Calculations: Gas-phase density functional theoretical (DFT) calculations of Mn(HSD*-COOH) and Mn(H_{ph}SD*-COOH) were performed using the Amsterdam Density Functional (ADF2002.02)[58,59] package on a home-built Linux cluster of sixty Intel processors running in parallel groups of 12. To simplify the calculation, the *tert*-butyl and methyl groups were removed from the xanthene spacer, and the cyclohexyl backbone was replaced with ethylenediamine. The generalized gradient approximation (GGA) was implemented by the use of Becke's exchange functional[60] and Perdew and Wang's correlation functional.[61] The basis set was of triple-zeta quality for manganese, oxygen, and nitrogen, with a double set of polarization functions for Mn and a single polarization set for O and N, and of double-zeta quality with single polarization set for carbon and hydrogen; the frozen core approximation was used for the 1s shell of C, N, and O and for the 1s, 2s, and 2p shells of Mn. Full geometry optimizations of the entire complexes were run at 0 K. All computations were carried out in the quintet spin state and the spin restriction was lifted. The molecular geometries and the spatial components of the resulting Kohn–Sham single-electron wave functions were visualized and analyzed using the software Molekel.[62,63]

Stopped-Flow UV-Vis Kinetic Measurements. Kinetic measurements were performed using a Hi-Tech Scientific (presently, TgK Scientific, Salisbury, Wiltshire, UK) SF-43 cryogenic double-mixing stopped-flow instrument equipped with stainless steel plumbing, a 1.00-cm stainless steel mixing cell with sapphire windows, and an anaerobic gas-flushing kit. The instrument was connected to an IBM computer with IS-2 Rapid Kinetics Software by Hi-Tech Scientific (presently TgK Scientific). The source of light was either a visible lamp combined with a monochromator or a xenon lamp combined with a diode array rapid scanning unit. Solutions of a manganese(III) complex and H_2O_2 were cooled to a preset temperature in the stopped-flow instrument before mixing. The temperature of the mixing cell was maintained to ±0.1 K, and the mixing time was 2–3 ms. The concentrations of the reactants were corrected for the 1:1 mixing ratio.

Stopped-Flow Kinetics: In a representative procedure, a gas-tight syringe was charged with Mn[H_{ph}SX*-OMe]Cl (5.0×10^{-5} M) in MeOH containing 2.5×10^{-4} M NaOH. A second gas-tight syringe was charged with 3.4×10^{-1} M H_2O_2 in MeOH containing 2.5×10^{-4} M NaOH. The stopped-flow spectrophotometer was charged with the solutions, and mixing was initiated by simultaneous injection of 0.1 mL of each solution to make the reactant concentrations 2.5×10^{-5} M and 1.7×10^{-1} M in manganese and H_2O_2, respectively. The solutions were cooled to the desired temperature prior to mixing and maintained at that temperature in a chilled heptane bath throughout the reaction. The reaction was monitored by UV/Vis spectroscopy. Spectra (350–700 nm) were acquired for 100 s at 0.5 s intervals. The kinetic traces obtained under the pseudo-first-order conditions over 3–5 half-lives were fit at single wavelengths with IS-2 Rapid Scanning Kinetic Software. In many cases, oxidation of the manganese(III) precursor by H_2O_2 was accompanied by decomposition of hydrogen peroxide. Unless stated otherwise, the resulting kinetic traces were fit using a monoexponential rate law that accounted for hydrogen peroxide decomposition with a slope given by Equation (1), where *m* is the effective zero-order rate constant of H_2O_2 decomposition.

$$A_t = A_\infty + mt - (A_\infty - A_t)^{-k_{obs}t} \quad (1)$$

The fit of experimental data to Equation (1), and the independence of k_{obs} on the concentration of MnL served as proof of the first-order behavior of the reactions in the Mn^{III} complex. A linear dependence of k_{obs} on the concentration of H_2O_2 served as proof of the first-order behavior of the reactions in hydrogen peroxide. Equation (2) was used to calculate the second-order rate constant *k*.

$$-d[Mn^{III}L]/(dt) = k_{obs}[Mn^{III}L] = k[Mn^{III}L][H_2O_2]$$
$$k = k_{obs}/[H_2O_2] \quad (2)$$

The values of *k* ($M^{-1}s^{-1}$) were determined at different temperatures and fit to the Eyring equation [Eq. (3)] to obtain the activation parameters ΔH^+ and ΔS^+.

$$\ln(k/T) = 23.76 + \Delta S^+ R^{-1} - \Delta H^+ (RT)^{-1} \quad (3)$$

Hydrogen Peroxide Disproportionation Reactions: Dismutation reactions were performed at room temperature in a sealed (PTFE septum) 20-mL reaction vial equipped with a magnetic stir bar and a capillary gas delivery tube linked to an inverted graduated burette filled with water. The reaction vial was charged with a stock solution of the corresponding catalyst in CH_2Cl_2 (1.0 mL). MeOH (0.5 mL) was added to the solution followed by the addition of H_2O_2 (790 μL, 8.22 mmol; 10.4 M 30% aq. solution). The reaction mixture was stirred vigorously. The time was set to zero immediately after addition of H_2O_2. The reaction was monitored volumetrically, and the amount of produced O_2 was calculated with the perfect gas equation assuming that $p = 1$ atm. The following amounts of catalyst were used to obtain the results listed in Table 1: Mn[HSD*tBu-COOH]Cl (**11**; 1.0 mL from a solution of 4.5 mg in 10 mL CH_2Cl_2; 0.000475 mmol) to give an average of 9.55 mL of O_2 in 1 h. Mn[H_{ph}SD*tBu-COOH]Cl (**12**; 1.0 mL from a solution of 5.2 mg in 10 mL CH_2Cl_2; 0.000475 mmol) to give 28.9 mL of O_2 in 1 h. The standard deviations on the turnover number measurements over 1 h are derived from at least three data points. The reaction conditions are the same as those used previously.[29]

Epoxidation of 2,2-Dimethylpropionic acid 4-vinylphenyl ester (**18**): A solution of 2,2-dimethylpropionic acid 4-bromophenyl ester (47.5 mM) and dodecane (23.75 mM) was prepared (i.e., 2,2-dimethylpropionic acid 4-bromophenyl ester (242.6 mg) and dodecane (101.1 mg) in dichloromethane (25 mL)). The oxidant solution was prepared by mixing 0.05 M $NaHPO_4$ (10 mL) with commercial

bleach (Clorox; 25 mL) and 1 M NaOH solution (1.0 mL). This solution was cooled to 0 °C. For each reaction, 0.5 mL of the catalyst solution was added to 0.5 mL of the solution of 2,2-dimethylpropionic acid 4-bromophenyl ester/dodecane and cooled to 0 °C; 1.0 mL of the oxidant solution was added to each reaction and stirred at room temperature. The reactions were calibrated at $t=0$, and examined by GC-MS at $t=1$ h and 3 h. The response factor of the substrate and epoxidation product relative to the internal standard of dodecane was determined and fitted with at least three points using a linear calibration curve. The calibration curve was used to determine the concentrations of the substrate and epoxide product, and it was used to calculate the corresponding turnover numbers based on the concentration of product. The GC-MS spectra were recorded on an Agilent Technologies 6890N Network housed at the MIT DCIF.

Acknowledgement

We gratefully acknowledge Julien Bachmann, and Matt Kanan for fruitful discussions. This work was supported by funding from the DOE (DE-FG02-05ER15745 (to D.G.N.) and DE-FG02-06ER15799 (to E.R.A.)). Stopped-flow instrumentation at Tufts was supported by the NSF-CRIF program (CHE-0639138).

Keywords: electron transfer · epoxidation · manganese · N,O ligands

[1] R. I. Cukier, D. G. Nocera, *Annu. Rev. Phys. Chem.* **1998**, *49*, 337.
[2] M. H. V. Huynh, T. J. Meyer, *Chem. Rev.* **2007**, *107*, 5004.
[3] J. M. Mayer, *Annu. Rev. Phys. Chem.* **2004**, *55*, 363.
[4] S. Hammes-Schiffer, *Acc. Chem. Res.* **2006**, *39*, 93.
[5] J. Rosenthal, J. M. Hodgkiss, E. R. Young, D. G. Nocera, *J. Am. Chem. Soc.* **2006**, *128*, 10474.
[6] T. A. Betley, Y. Surendranath, M. V. Childress, G. E. Alliger, R. Fu, C. C. Cummins, D. G. Nocera, *Philos. Trans. R. Soc. B* **2008**, *363*, 1293.
[7] J. Rosenthal, D. G. Nocera, *Acc. Chem. Res.* **2007**, *40*, 543.
[8] J. Rosenthal, D. G. Nocera, *Prog. Inorg. Chem.* **2007**, *55*, 483.
[9] T. A. Betley, Q. Wu, T. Van Voorhis, D. G. Nocera, *Inorg. Chem.* **2008**, *47*, 1849.
[10] J. Stubbe, D. G. Nocera, C. S. Yee, M. C. Y. Chang, *Chem. Rev.* **2003**, *103*, 2167.
[11] C. J. Fecenko, T. J. Meyer, H. H. Thorp, *J. Am. Chem. Soc.* **2006**, *128*, 11020.
[12] S. Y. Reece, M. R. Seyedsayamdost, J. Stubbe, D. G. Nocera, *J. Am. Chem. Soc.* **2007**, *129*, 8500.
[13] S. Y. Reece, M. R. Seyedsayamdost, J. Stubbe, D. G. Nocera, *J. Am. Chem. Soc.* **2007**, *129*, 13828.
[14] T. Irebo, O. Johansson, L. Hammarstrom, *J. Am. Chem. Soc.* **2008**, *130*, 9194.
[15] S. Y. Reece, J. M. Hodgkiss, J. Stubbe, D. G. Nocera, *Philos. Trans. R. Soc. B* **2006**, *361*, 1351.
[16] P. A. Frey, A. D. Hegeman, G. H. Reed, *Chem. Rev.* **2006**, *106*, 3302.
[17] C.-Yu Yeh, C. J. Chang, D. G. Nocera, *J. Am. Chem. Soc.* **2001**, *123*, 1513.
[18] L. L. Chng, C. J. Chang, D. G. Nocera, *Org. Lett.* **2003**, *5*, 2421.
[19] S.-Y. Liu, D. G. Nocera, *J. Am. Chem. Soc.* **2005**, *127*, 5278.
[20] J. D. Soper, S. V. Kryatov, E. V. Rybak-Akimova, D. G. Nocera, *J. Am. Chem. Soc.* **2007**, *129*, 5069.
[21] C. J. Chang, L. L. Chng, D. G. Nocera, *J. Am. Chem. Soc.* **2003**, *125*, 1866.
[22] A. P. Olcott, G. Tocco, J. Tian, D. Zekzer, J. Fukuto, L. Ignarro, D. L. Kaufman, *Diabetes* **2004**, *53*, 2574.
[23] S. R. Doctrow, K. Huffman, C. B. Marcus, G. Tocco, E. Malfroy, C. A. Adinolfi, H. Kruk, K. Baker, N. Lazarowych, J. Mascarenhas, B. Malfroy, *J. Med. Chem.* **2002**, *45*, 4549.
[24] S. R. Doctrow, C. Adinolfi, M. Baudry, K. Huffman, B. Malfroy, C. B. Marcus, S. Melov, K. Pong, Y. Rong, J. L. Smart, G. Tocco in *Critical Reviews of Oxidative Stress and Aging: Advances in Basic Science Diagnostics, and Intervention, Vol. 2* (Eds.: R. G. Cutler, H. Rodriquez), World Scientific, New Jersey, **2003**, p. 1324.
[25] M. C. McDonald, R. d'Emmanuele di Villa Bianca, N. S. Wayman, A. Pinto, M. A. Sharpe, S. Cuzzocrea, P. K. Chatterjee, C. Thiemermann, *Eur. J. Pharmacol.* **2003**, *466*, 181.
[26] K. Baker, C. B. Marcus, K. Huffman, H. Kruk, B. Malfroy, S. R. Doctrow, *J. Pharmacol. Exp. Ther.* **1998**, *284*, 215.
[27] D. Decraene, K. Smaers, D. Gan, T. Mammone, M. Matusi, D. Maes, L. Declercq, M. Garmyn, *J. Invest. Dermatol.* **2004**, *122*, 484.
[28] J. D. Soper, S. V. Kryatov, E. V. Rybak-Akimova, D. G. Nocera, *J. Am. Chem. Soc.* **2007**, *129*, 5069.
[29] S.-Y. Liu, J. D. Soper, J. Y. Yang, E. V. Rybak-Akimova, D. G. Nocera, *Inorg. Chem.* **2006**, *45*, 7572.
[30] E. B. Schwartz, C. B. Knobler, D. J. Cram, *J. Am. Chem. Soc.* **1992**, *114*, 10775.
[31] J. Y. Yang, D. G. Nocera, *J. Am. Chem. Soc.* **2007**, *129*, 8192.
[32] R. Davydov, T. M. Makris, V. Kofman, D. E. Werst, S. G. Sligar, B. M. Hoffman, *J. Am. Chem. Soc.* **2001**, *123*, 1403.
[33] F. Ogliaro, S. P. de Visser, S. Cohen, P. K. Sharma, S. Shaik, *J. Am. Chem. Soc.* **2002**, *124*, 2806.
[34] J. T. Groves, Y. Watanabe, *J. Am. Chem. Soc.* **1988**, *110*, 8443.
[35] J. Y. Yang, J. Bachmann, D. G. Nocera, *J. Org. Chem.* **2006**, *71*, 8706.
[36] I. V. Khavrutskii, D. G. Musaev, K. Morokuma, *Inorg. Chem.* **2005**, *44*, 306.
[37] Y. G. Abashkin, S. K. Burt, *Inorg. Chem.* **2005**, *44*, 1425.
[38] Y. G. Abashkin, S. K. Burt, *J. Phys. Chem. B* **2004**, *108*, 2708.
[39] M. Haumann, P. Liebisch, C. Muller, M. Barra, M. Grabolle, H. Dau, *Science* **2005**, *310*, 1019.
[40] K. N. Ferreira, T. M. Iverson, K. Maghlaoui, J. Barber, S. Iwata, *Science* **2004**, *303*, 1831.
[41] S. Iwata, J. Barber, *Curr. Opin. Struct. Biol.* **2004**, *14*, 447.
[42] J. Yano, J. Kern, K. Sauer, M. J. Latimer, Y. Pushkar, J. Biesiadka, B. Loll, W. Saenger, J. Messinger, A. Zouni, V. Yachandra, *Science* **2006**, *314*, 821.
[43] B. Loll, J. Kern, W. Saenger, A. Zouni, J. Biesiadka, *Nature* **2005**, *438*, 1040.
[44] J. Barber, *Inorg. Chem.* **2008**, *47*, 1700.
[45] J. Yano, V. K. Yachandra, *Inorg. Chem.* **2008**, *47*, 1711.
[46] J. M. Peloquin, K. A. Campbell, D. W. Randall, M. A. Evanchik, V. L. Pecoraro, W. H. Armstrong, R. D. Britt, *J. Am. Chem. Soc.* **2000**, *122*, 10926.
[47] V. L. Pecoraro, M. J. Baldwin, M. T. Caudle, W.-Y. Hsieh, N. A. Law, *Pure Appl. Chem.* **1998**, *70*, 925.
[48] J. P. McEvoy, G. W. Brudvig, *Chem. Rev.* **2006**, *106*, 4455.
[49] N. S. Lewis, D. G. Nocera, *Proc. Nat. Acad. Sci. U. S. A.* **2006**, *103*, 15729.
[50] D. G. Nocera, *Dædulus* **2006**, *135*, 112.
[51] R. Eisenberg, D. G. Nocera, *Inorg. Chem.* **2005**, *44*, 6799.
[52] M. I. Hoffert, K. Caldeira, A. K. Jain, E. F. Haites, L. D. D. Harvey, S. D. Potter, M. E. Schlesinger, S. H. Schneider, R. G. Watts, T. M. L. Wigley, D. J. Wuebbles, *Nature* **1998**, *395*, 881.
[53] W. L. F. Armarego, D. D. Perrin, *Purification of Laboratory Chemicals, 4th ed.*, Butterworth-Heinemann, Oxford, **1966**.
[54] E. B. Schwartz, C. B. Knobler, D. J. Cram, *J. Am. Chem. Soc.* **1992**, *114*, 10775.
[55] J. Y. Yang, D. G. Nocera, *J. Am. Chem. Soc.* **2007**, *129*, 8192.
[56] C. J. Chang, L. L. Chng, D. G. Nocera, *J. Am. Chem. Soc.* **2003**, *125*, 1866.
[57] S.-Y. Liu, D. G. Nocera, *J. Am. Chem. Soc.* **2005**, *127*, 5278.
[58] G. te Velde, F. M. Bickelhaupt, A. J. A. van Gisbergen, C. Fonseca Guerra, E. J. Baerends, J. G. Snijders, T. J. Ziegler, *Comput. Chem.* **2001**, *22*, 931.
[59] C. Fonseca Guerra, J. G. Snijders, G. te Velde, E. J. Baerends, *Theor. Chem. Acc.* **1998**, *99*, 391.
[60] A. D. Becke, *Phys. Rev. A* **1998**, *38*, 3098.
[61] J. P. Perdew, J. A. Chevary, S. H. Vosko, K. A. Jackson, M. R. Pederson, D. J. Singh, C. Fiolhais, *Phys. Rev. B* **1992**, *46*, 6671.
[62] Molekel v. 4.2/3, P. Flükiger, H. P. Lüthi, S. Portmann, J. Weber, Swiss Center for Scientific Computing, Manno, 2000–2002.
[63] S. Portmann, H. P. Lüthi, *Chimia* **2000**, *54*, 776.

Received: May 25, 2008
Revised: September 11, 2008
Published online on November 4, 2008

